Performance Comparison of a Second-order adaptive IIR Notch Filter based on Plain Gradient Algorithm

Wuthiporn Loedwassana, Non-member

ABSTRACT

This paper presents performance analysis of a second-order adaptive IIR notch filter with constrained poles and zeros in direct form II structure that is adapted by algorithms of indirect and direct frequency estimations based on plain gradient. In this work, the steady-state bias properties and stability bounds of both algorithms are derived in closed form. The simulated processes are performed in order to verify the analytical results. Furthermore, these results of the proposed filter are also compared with those results of the direct form I adaptive IIR notch filter under the same parameters. It has been revealed that the steady-state bias properties of the direct form II structure were lower than those of the direct form I structure.

Keywords: Adaptive IIR notch filter, IIR direct form II, Gradient-based algorithm

1. INTRODUCTION

An adaptive notch filter has been employed in many applications such as frequency estimation, sinusoidal enhancement, periodical noise cancellation, and so on. It is well-known that an adaptive infinite impulse response (IIR) notch filter is better than an adaptive finite impulse response (FIR) notch filter in performance and computational complexity for the same notch bandwidth. An adaptive IIR notch filter with constrained poles and zeros (IIR-ANF) has been proposed in the literature. The N-order IIR-ANF in direct form I structure whose coefficients are updated by the recursive prediction error (RPE) algorithm was proposed by [1]. The plain gradient (PG) algorithm which adjusts a coefficient of a second-order IIR-ANF in direct form I (ANF-I) structure has been proposed by [2] for frequency estimation of sinusoidal signals in noise. The ANF-I with the least mean p-power (LMP) adaptive algorithm was employed for cancelling 60 Hz power-line signal that interferes in an electrocardiogram (ECG) signal [3]. Moreover, Xiao had proposed the steady-state performance analyses of the PG algorithm [4] and the sign algorithm (SA) [5] that both algorithms adapt the coefficient of the filter. Some applications of the ANF-I have been presented in many articles such as a howling phenomenon in an audio power amplifier system is suppressed by using the filter with the SA adaptive algorithm [6] and a frequency tracking in optical Doppler tomography by using the filter with the PG algorithm is employed to study subsurface blood flows of biological tissues [7].

As mentioned above that, these algorithms adapt the coefficients in order to adjust notch frequencies of the filter coincident to the input sinusoidal frequency, respectively. Therefore, the algorithms are so called the indirect frequency estimation. Recently, the direct frequency estimation based on plain gradient (DPG) algorithm which adapts directly notch frequency of the filter was proposed by [8] and the steady-state property of the algorithm was also derived. Furthermore, Punchalard [9] had proposed a new error criterion of the filter in order to increase convergent speed of the adaptive algorithm. In this work, the indirect frequency estimation based on plain gradient (IPG) and DPG algorithms for adapting the filter with such a criterion were presented and the steady-state properties of the algorithms were also analysed. Since such a filter structure which is adapted by the plain gradient algorithms provides inherent bias in steady state of the algorithms, the notch frequency of the filter is incorrect to the input sinusoidal frequency. In order to solve the bias, the unbiased plain gradient (UPG) algorithms for such a filter structure were proposed by [10, 11] that both give good performance in the steady state. However, the UPG algorithms produce local minima in the error function. Therefore, if initial coefficient value of the filter is not proper situation, the algorithms cannot adapt the coefficient converged to the optimum solution.

For a second-order IIR-ANF in direct form II (ANF-II) structure, it has been developed and proposed in the literature as well. The ANF-II which its coefficient is updated by the Gauss-Newton (GN) algorithm was presented for the retrieval of sinusoidal signal in noise [12]. Moreover, such a filter with the constrained least mean-square (CLMS) adaptive algorithm has been applied for removing a power-line

Manuscript received on November 8, 2016 ; revised on January 16, 2017.

The authors is with Department of Telecommunication Engineering, Mahanakorn University of Technology, Bangkok, Thailand, E-mail : wuthipor@mut.ac.th

noise from an electroencephalography (EEG) signal [13]. Recently, Lim [14] had proposed the ANF-II in modified form with the IPG adaptive algorithm in order to improve performance of the filter. Furthermore, [15] had proposed the ANF-II in cascade format with the DPG adaptive algorithm for estimate and tracking sinusoidal frequency in noise.

Since the ANF-II structure which the poles precede the zeros, the poles enhance the signal to noise ratio (SNR) of the system leaded to reducing the bias in the system [14]. From literature surveys, the steady-state performance of the filter with the plain-gradient adaptive algorithm was not presented in detailed analysis. Therefore, this paper proposes the steady-state performance analysis of the filter that is adapted by the IPG and DPG algorithms. In this work, the steady-state bias properties will be investigated in closed forms. Moreover, the stability bounds of both algorithms are also derived. In addition, the simulation processes will be demonstrated to confirm the theoretical analyses.

The paper is organized as follows. Section 2 introduces the ANF-II structure. The steady-state performance analysis of the ANF-II which is adapted by IPG algorithm will be considered in section 3. Section 4 describes the steady-state performance of the filter with DPG adaptive algorithm. The stability bounds of both algorithms are derived in section 5. In section 6, the analytical and simulated results will be compared. Finally, the conclusion is provided in section 7.

2. ADAPTIVE IIR NOTCH FILTER IN DIRECT FORM II STRUCTURE

A second-order adaptive IIR notch filter with constrained poles and zeros in direct form II (ANF-II) structure which is the same transfer function as a second-order IIR-ANF in direct form I (ANF-I) structure is given by

$$H(z) = \frac{1 + az^{-1} + z^{-2}}{1 + \rho az^{-1} + \rho^2 z^{-2}}, \tag{1}$$

where $0 < \rho < 1$ is a pole radius which controls notch bandwidth of the filter. a is an estimated coefficient whose true value can be calculated by $a_o = 2cos\omega_\circ$ and $\omega_\circ$ denotes an input sinusoidal frequency [4]. Output equation of the filter which is different from the ANF-I is shown in detail as follows:

$$y(n) = u(n) + a(n)u(n-1) + u(n-2) \tag{2}$$

and

$$u(n) = x(n) - \rho a(n)u(n-1) - \rho^2 u(n-2), \tag{3}$$

where $y(n)$ and $x(n)$ are the output and input of the filter, respectively. It is assumed that the input signal is a sinusoid plus a zero-mean white Gaussian process as

$$x(n) = Acos(\omega_o n + \theta) + v(n), \tag{4}$$

where A denotes a sinusoidal amplitude, θ is a random variable of phase that distributes a uniform probability density function (PDF) over (π, π). $v(n)$ is an additive white Gaussian noise (AWGN) signal that its variance is σ_v^2 and n denotes system time index.

3. INDIRECT FREQUENCY ESTIMATION ADAPTIVE ALGORITHM

An adaptive algorithm with indirect frequency estimation based on plain gradient (IPG) which updates the coefficient of the ANF-II is given by

$$a(n+1) = a(n) + \frac{\mu}{2}\left\{-\hat{\nabla}_a(n)\right\}, \tag{5}$$

where $\hat{\nabla}_a(n)$ is the gradient estimation that can be derived in the solution as $\hat{\nabla}_a(n) = \frac{\partial y^2(n)}{\partial a} \approx 2y(n)s_a(n)$ and $s_a(n) = \frac{\partial y(n)}{\partial a} \approx (1-\rho)u(n-1)$. After these solutions are substituted into (5), the IPG algorithm can be simply shown as

$$a(n+1) = a(n) - \mu y(n)s_a(n), \tag{6}$$

where μ is a step-size parameter that controls convergent speed and stability of the algorithm. $y(n)$ which is output signal of the filter denotes an error signal of the algorithm and $s_a(n)$ is a gradient signal whose transfer function is expressed in form

$$G_a(z) = \frac{S_a(z)}{X(z)} = \frac{(1-\rho)z^{-1}}{1 + \rho az^{-1} + \rho^2 z^{-2}}. \tag{7}$$

To investigate bias in steady state of the algorithm, (6) is reformed in equation of coefficient difference in the mean sense, that is

$$E[\delta_a(n+1)] = E[\delta_a(n)] - \mu E[y_a(n)s_a(n)], \tag{8}$$

where $\delta_a(n)$ is an instantaneous coefficient difference that is defined by $a(n)$ - a_o. At steady state, the value of the instant coefficient a(n) will be close to its true value a_o. Therefore, using the Taylor series estimation, the transfer function of (1) in vicinity of the true value can be approximated as [4]

$$H_a(e^{j\omega_o}) \approx \delta_a B e^{-j\phi} - \rho\delta_a^2 B^2 e^{-j2\phi}, \tag{9}$$

$$B = \frac{1}{(1-\rho)\sqrt{(1+\rho)^2 - \rho a_o^2}}, \tag{10}$$

$$\phi = \begin{cases} \tan^{-1}\left[\frac{(1+\rho)\sin\omega_o}{(1-\rho)\cos\omega_o}\right] & , \omega_o \le \frac{\pi}{2} \\ \pi + \tan^{-1}\left[\frac{(1+\rho)\sin\omega_o}{(1-\rho)\cos\omega_o}\right] & , \omega_o > \frac{\pi}{2} \end{cases}, \tag{11}$$

where B and ϕ are magnitude and phase responses of the $H_a(e^{j\omega_o})$ function. Similarly, the transfer function of (7) in the vicinity of the true coefficient can be expressed as

$$G_a(e^{j\omega_o}) \approx (1-\rho)[1-\rho H_a(e^{j\omega_o})]Be^{-j\phi}. \quad (12)$$

By applying (4) into (9) and (12), the error and gradient signals in steady state can be respectively derived in the solutions as follows:

$$\begin{aligned} &y_a(n) = AB\delta_a(n)\cos(\omega_o n+\theta-\phi) \\ &-\rho AB^2\delta_a^2(n)\cos(\omega_o n+\theta-2\phi)+v_1(n), \end{aligned} \quad (13)$$

$$\begin{aligned} &s_a(n) = (1-\rho)AB\cos(\omega_o n+\theta-\phi) \\ &-\rho(1-\rho)AB^2\delta_a(n)\cos(\omega_o n+\theta-2\phi) \\ &+\rho^2(1-\rho)AB^3\delta_a^2(n)\cos(\omega_o n+\theta-3\phi)+v_2(n), \end{aligned} \quad (14)$$

where $v_1(n)$ and $v_2(n)$ are zero-mean noise signals at the output of the $H_a(e^{j\omega_o})$ and $G_a(e^{j\omega_o})$ filters, respectively. Both signals are originated by the $v(n)$ signal. The $v_1(n)$ signal has the same variance σ_1^2 as (10) in [4] while variance of the $v_2(n)$ signal can be investigated by mean of residual theorem, that is

$$\begin{aligned} &\sigma_2^2 = E[v_2^2(n)] = \tfrac{1}{j2\pi}\oint G_a(z)G_a(z^{-1})\sigma_v^2\tfrac{dz}{z} \\ &= \tfrac{1-\rho}{1+\rho}\ \tfrac{(1+\rho^2)\sigma_v^2}{(1+\rho^2)^2-\rho^2 a_o^2}. \end{aligned} \quad (15)$$

A and ω_o are constant parameters and θ is a random variable. Second, the algorithm adapts slowly the coefficient in order that the sinusoidal signal is statistically independent with the coefficient difference. Third, the $v_1(n)$ and $v_2(n)$ are uncorrelated to the sinusoidal signal and coefficient difference, respectively. Fourth, Both $v_1(n)$ and $v_2(n)$ are jointly Gaussian distributed. Furthermore, the term of $\delta_a^k(k \geqslant 3)$ can be neglected because they are actually much smaller than both $E[\delta_a(n)]$ and $E[\delta_a^2(n)]$ [4, 11]. Therefore, the coefficient difference in the mean can be simplified and expressed by

$$\begin{aligned} &E[\delta_a(n+1)] = (1-\mu\varphi_1)E[\delta_a(n)] \\ &+\mu\varphi_2 E[\delta_a^2(n)]-\mu r_{12}, \end{aligned} \quad (16)$$

where defining $\varphi_1 = (1-\rho)\frac{A^2}{2}B^2$,$\varphi_2 = \rho(1-\rho)A^2B^3\cos\phi$ and r_12 denotes the correlation of the noise signals that can be found in the solution to be

$$\begin{aligned} &r_{12} = E[v_1(n)v_2(n)] = \tfrac{1}{j2\pi}\oint H_a(z)G_a(z^{-1})\sigma_v^2\tfrac{dz}{z} \\ &= \tfrac{(1-\rho)^2}{1+\rho}\ \tfrac{a_o\sigma_v^2}{(1+\rho^2)^2-\rho^2 a_o^2}. \end{aligned} \quad (17)$$

When (16) has been sequentially considered in long time, the following conditions can be satisfied as $\lim_{n\to\infty} E[\delta_a(n)] = \lim_{n\to\infty} E[\delta_a(n+1)] = E[\delta_a(\infty)]$ and $\lim_{n\to\infty} E[\delta_a^2(n)] = \lim_{n\to\infty} E[\delta_a^2(n+1)] = E[\delta_a^2(\infty)]$. Therefore, the steady-state bias estimation of the IPG algorithm which adjusts the coefficient of the ANF-II can be derived as

$$E[\delta_a(\infty)] = \frac{\varphi_2}{\varphi_1}E[\delta_a^2(\infty)] - \frac{r_{12}}{\varphi_1}. \quad (18)$$

It has implied that the bias expression is mainly composed of mean square error (MSE) of coefficient term and correlation term.

To obtain the instant MSE equation, (8) is then considered by squaring both sides of the equation, that is

$$\begin{aligned} &E[\delta_a^2(n+1)] = E[\delta_a^2(n)] - 2\mu E[\delta_a(n)y_a(n)s_a(n)] \\ &+\mu^2 E[y_a^2(n)s_a^2(n)]. \end{aligned} \quad (19)$$

Taking (13) and (14) replacing in (19), the analytical process is arranged by using above assumptions and additional assumption that $E[v_1^2(n)v_2^2(n)]$ can be calculated by mean of the Gaussian moment factoring theorem. Therefore, the instant MSE in simplified form can be shown as follows:

$$\begin{aligned} &E[\delta_a^2(n+1)] = (1-2\mu\varphi_1+\mu^2\eta_1)E[\delta_a^2(n)] \\ &+(\mu^2\eta_2-2\mu r_{12})E[\delta_a(n)]+\mu^2\eta_3, \end{aligned} \quad (20)$$

where

$$\begin{aligned} &\eta_1 = \tfrac{3}{2}\varphi_1^2+\tfrac{A^2}{2}B^2\sigma_2^2-4\varphi_2 r_{12} \\ &+\rho(1-\rho)(2\varphi_2\cos\phi-\rho B\varphi_1)B\sigma_1^2, \end{aligned} \quad (21)$$

$$\eta_2 = 4\varphi_1 r_{12}-(1-\rho)\varphi_2\sigma_1^2, \quad (22)$$

$$\eta_3 = (1-\rho)\varphi_1\sigma_1^2+\sigma_1^2\sigma_2^2+2r_{12}^2. \quad (23)$$

After (20) is considered as above conditions in long time, the steady-state MSE of the coefficient can be solved as

$$E[\delta_a^2(\infty)] = \frac{\mu\eta_3+r_{12}(2r_{12}-\mu\eta_2)/\varphi_1}{2\varphi_1-\mu\eta_1+\varphi_2(2r_{12}-\mu\eta_2)/\varphi_1}. \quad (24)$$

Substituting (24) back to (18), the steady-state bias of the algorithm can be derived in closed form to be

$$E[\delta_a(\infty)] = \frac{\mu(\varphi_2\eta_3+r_{12}\eta_1)-2\varphi_1 r_{12}}{\varphi_1(2\varphi_1-\mu\eta_1)+\varphi_2(2r_{12}-\mu\eta_2)}. \quad (25)$$

4. DIRECT FREQUENCY ESTIMATION ADAPTIVE ALGORITHM

A direct frequency estimation algorithm which updates notch frequency of the ANF-II can be given in format

$$\omega(n+1) = \omega(n)+\frac{\mu}{2}\left\{-\hat{\nabla}_\omega(n)\right\}. \quad (26)$$

The algorithm is based on the plain gradient estimation. Namely, the solution of the gradient estimation can be derived by $\hat{\nabla}_\omega(n) = \frac{\partial y^2(n)}{\partial\omega} \approx 2y(n)s_\omega(n)$ and $s_\omega(n) = \frac{\partial y(n)}{\partial\omega} \approx (1-\rho)b(n)u(n-1)$. Therefore, it is so called the direct frequency estimation based on plain gradient (DPG) algorithm. Substituting these solutions back to (26), the DPG adaptive algorithm can be simply expressed by

$$\omega(n+1) = \omega(n)-\mu y(n)s_\omega(n), \quad (27)$$

where $s_\omega(n)$ denotes a gradient signal of the algorithm that its transfer function can be written in form

$$G_\omega(z) = \frac{S_\omega(z)}{X(z)} = \frac{(1-\rho)bz^{-1}}{1+\rho az^{-1}+\rho^2 z^{-2}}, \quad (28)$$

where defining $b = 2sin\omega$ and ω is an estimated notch frequency by the algorithm. It has been noted that (28) is similar format of (7).

For investigating a steady-state property of the algorithm, it can be processed in the same manner as previous section by considering (27) formed in a frequency difference equation in the mean sense, that is

$$E[\delta_\omega(n+1)] = E[\delta_\omega(n)] - \mu E[y_\omega(n)s_\omega(n)], \quad (29)$$

where $\delta_\omega(n)$ denotes an instantaneous frequency difference that is defined by $\omega(n) - \omega_o$ and ω_o is true notch frequency. At steady state, the instantly estimated notch frequency $\omega(n)$ will be close to its true notch. Therefore, the transfer function of (1) in vicinity of the true notch can be approximated as [8]

$$\begin{aligned} H_\omega(e^{j\omega_o}) \approx\ & b_o\delta_\omega Be^{-j\phi} + \tfrac{b_o}{2}\cot\omega_o\delta_\omega^2 Be^{-j\phi} \\ & -\rho b_o^2\delta_\omega^2 B^2 e^{-j2\phi}. \end{aligned} \quad (30)$$

Similarly, the transfer function of (28) in the vicinity of the true notch can be expressed as

$$G_\omega(e^{j\omega_o}) \approx (1-\rho)b_o[D(e^{j\omega_o}) - \rho H_\omega(e^{j\omega_o})]Be^{-j\phi}, \quad (31)$$

where $D(e^{j\omega_o}) = 1 - \frac{\delta_\omega^2}{2} + (1-\rho b_o\delta_\omega Be^{-j\phi})\delta_\omega\cot\omega_o$ and $b_o = 2sin\omega_o$. When (4), (30) and (31) are considered, the error and gradient signals in steady state can be respectively found in the solutions as follows:

$$\begin{aligned} y_\omega(n) =\ & b_o AB\delta_\omega(n)\cos(\omega_o n+\theta-\phi) \\ & +\tfrac{b_o}{2}AB\cot\omega_o\delta_\omega^2(n)\cos(\omega_o n+\theta-\phi) \\ & -\rho b_o^2 AB^2\delta_\omega^2(n)cos(\omega_o n+\theta-2\phi) + v_3(n), \end{aligned} \quad (32)$$

$$\begin{aligned} s_\omega(n) =\ & (1-\rho)b_o AB\cos(\omega_o n+\theta-\phi) \\ & +(1-\rho)b_o AB\cot\omega_o\delta_\omega(n)cos(\omega_o n+\theta-\phi) \\ & -(1-\rho)\tfrac{b_o}{2}AB\delta_\omega^2(n)cos(\omega_o n+\theta-\phi) \\ & -\rho(1-\rho)b_o^2 AB^2\delta_\omega(n)cos(\omega_o n+\theta-2\phi) \\ & -\tfrac{3\rho}{2}(1-\rho)b_o^2 AB^2\cot\omega_o\delta_\omega^2(n)cos(\omega_o n+\theta-2\phi) \\ & +\rho^2(1-\rho)b_o^3 AB^3\delta_\omega^2(n)cos(\omega_o n+\theta-3\phi) \\ & +v_4(n), \end{aligned} \quad (33)$$

where $v_3(n)$ and $v_4(n)$ are zero-mean noise signals at the output of the $H_\omega(e^{j\omega_o})$ and $G_\omega(e^{j\omega_o})$ filters, respectively. Both signals are also originated by the $v(n)$ signal. Variance of the $v_3(n)$ signal is identical to the $v_1(n)$ signal ($\sigma_3^2 = \sigma_1^2$) while variance of the $v_4(n)$ signal can be found in solution to be $\sigma_4^2 = E[v_4^2(n)] = b_o^2\sigma_2^2$. Furthermore, the correlation of the $v_3(n)$) and $v_4(n)$) signals can be derived in the solution as $r_3^4 = E[v_3(n)v_4(n)] = b_o r_{12}$. Taking (32) and (33) replacing back to (29), the instantaneous frequency difference equation in the mean is then analysed by using previous assumptions. Therefore, the simplified form of the equation can be shown as

$$\begin{aligned} E[\delta_\omega(n+1)] =\ & (1-\mu b_o^2\varphi_1)E[\delta_\omega(n)] \\ & +\mu b_o^2\varphi_3 E[\delta_\omega^2(n)] - \mu b_o r_{12}, \end{aligned} \quad (34)$$

and defining the parameter of $\varphi_3 = b_o\varphi_2 - \frac{3\varphi_1}{2}\cot\omega_o$. Considering (34) in long time such as previous conditions, the steady-state bias of the algorithm can be derived in a general form to be

$$E[\delta_\omega(\infty)] = \frac{\varphi_3}{\varphi_1}E[\delta_\omega^2(\infty)] - \frac{r_{12}}{b_o\varphi_1}, \quad (35)$$

where $E[\delta_\omega^2(\infty)]$ denotes MSE of notch frequency at steady state. It is seen that the bias equation of the DPG algorithm consists of the MSE and correlation terms as well.

To obtain an instant MSE equation of the algorithm, (29) is then considered in square form, that is

$$\begin{aligned} E[\delta_\omega^2(n+1)] =\ & E[\delta_\omega^2(n)] - 2\mu E[\delta_\omega(n)y_\omega(n)s_\omega(n)] \\ & +\mu^2 E[y_\omega^2(n)s_\omega^2(n)]. \end{aligned} \quad (36)$$

When (32) and (33) are taken for substituting into (36) and using the same assumptions as previous section, the instant MSE can be analysed to provide the solution as follows:

$$\begin{aligned} E[\delta_\omega^2(n+1)] =\ & (1-2\mu b_o^2\varphi_1+\mu^2 b_o^2\eta_4)E[\delta_\omega^2(n)] \\ & +(\mu^2 b_o^2\eta_5 - 2\mu b_o r_{12})E[\delta_\omega(n)] \\ & +\mu^2 b_o^2\eta_3, \end{aligned} \quad (37)$$

where

$$\begin{aligned} \eta_4 =\ & b_o^2\eta_1 - (1-\rho)(1-\cot^2\omega_o)\varphi_1\sigma_1^2 \\ & +\left(6\varphi_1 r_{12} - \tfrac{5(1-\rho)}{2}\varphi_2\sigma_1^2\right)b_o\cot\omega_o \end{aligned} \quad (38)$$

and

$$\eta_5 = b_o\eta_2 + 2(1-\rho)\varphi_1\sigma_1^2\cot\omega_o. \quad (39)$$

Considering (37) in long time leaded to the steady-state MSE equation, its solution can be derived as

$$E[\delta_\omega^2(\infty)] = \frac{\mu b_o^2\eta_3 + r_{12}(2r_{12}-\mu b_o\eta_5)/\varphi_1}{b_o^2(2\varphi_1-\mu\eta_4) + b_o\varphi_3(2r_{12}-\mu b_o\eta_5)/\varphi_1}. \quad (40)$$

It has shown that the steady-state MSE format of DPG algorithm is similar to the format of IPG algorithm in (24). Substituting (40) back to (35) and simplifying, the steady-state bias in closed form of the algorithm can be given by

$$E[\delta_\omega(\infty)] = \frac{\mu(b_o\varphi_3\eta_3 + r_{12}\eta_4) - 2\varphi_1 r_{12}}{b_o\varphi_1(2\varphi_1-\mu\eta_4) + \varphi_3(2r_{12}-\mu b_o\eta_5)}. \quad (41)$$

It has implied that the steady-state bias properties of both algorithms as shown in (25) and (41) are functions of many parameters such as a step size, a pole radius, a sinusoidal frequency and signal to noise ratio (SNR) at input of the filter.

5. STABILITY BOUND ANALYSIS

For an adaptive IIR notch filter, since ρ is the parameter that controls poles of the filter and μ controls convergent speed of the algorithm, both are the dominant parameters that govern stability of the adaptive filter. Because natural behaviour of an adaptive IIR algorithm is nonlinear, it is difficult to investigate the accurate solution of the stability boundary. However, the stability bound can be estimated by mean of the mean square error equation [4, 11].

Considering (20) for the IPG algorithm and (37) for the DPG algorithm, the first terms are the most significant to assure the convergence of the algorithms in the mean square sense [4, 11]. Therefore, $|1 - 2\mu\rho_1 + \mu^2\eta_1| < 1$ and $|1 - 2\mu b_o^2\varphi_1 + \mu^2 b_o^2\eta_4| < 1$ must be satisfied in order to confirm their convergences. Thus, the stability bounds on the step-size parameter of the IPG and DPG algorithms can be given in (42) and (43), respectively

$$0 < \mu < \frac{\varphi_1}{\eta_1}, \tag{42}$$

$$0 < \mu < \frac{\varphi_1}{\eta_4}. \tag{43}$$

It is revealed that the upper bounds are functions of the pole radius, input frequency and SNR value.

6. ANALYTICAL AND SIMULATED RESULTS

To verify the steady-state bias behaviours of the theoretical analyses, this section presents the comparisons of the analytical and simulated results leaded to confirming the performances of the proposed IPG (6) and DPG (27) algorithms that adapt the ANF-II. Moreover, these results will be also compared with those results of the IPG [4] and DPG [8] algorithms that adapt the ANF-I under the same parameters. These will be processed under assumption of a properly small step-size.

To obtain the simulated results of the steady-state bias properties, the ensemble average of 100 runs will be calculated. In addition, each run employs the input signal with 100,000 samples in order that their estimations reach to the steady state. Furthermore, analytically stability bounds of the proposed algorithms will be also verified by their simulation results.

6.1 Bias Behaviors of IPG Algorithms

The bias versus the input sinusoidal frequency of the proposed IPG algorithm that adapts the coefficient of the ANF-II and the IPG algorithm [4] that adapts the coefficient of the ANF-I under the same parameters are demonstrated in Fig. 1 (a). To achieve the compared results, the parameters are defined as follows: $\mu = 5 \times 10^{-5}$, $\rho = 0.85$, SNR = 5dB and $\theta = \pi/10$. Fig. 1 (b) shows the bias versus the step size of the algorithms by defining the parameters to be $\omega_o = 0.2\pi$, $\rho = 0.85$, SNR = 5dB and $\theta = \pi/10$. Fig. 1 (c) depicts the bias versus the pole radius of both filters that the coefficients are updated by their algorithms. To obtain the compared results, the parameters are determined in values of $\omega_o = 0.2\pi$, $\mu = 5 \times 10^{-5}$, SNR = 5dB and $\theta = \pi/10$. Furthermore, the bias versus the SNR is shown in Fig. 1 (d) by defining the parameters as follows: $\omega_o = 0.2\pi$, $\mu = 5 \times 10^{-5}$, $\rho = 0.85$ and $\theta = \pi/10$.

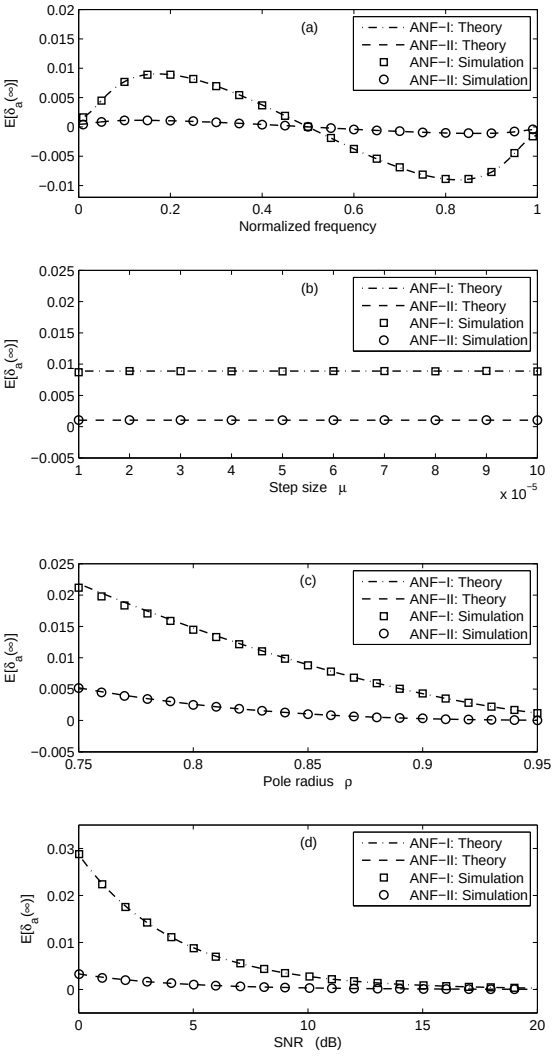

Fig. 1: *Steady-state Performances of the IPG Algorithms. (a) Bias versus Input sinusoidal Frequency. (b) Bias versus Step Size. (c) Bias versus Pole Radius. (d) Bias versus SNR.*

As shown in Fig. 1 (a) to Fig. 1 (d), these have been revealed that the steady-state biases of the ANF-II whose coefficient is adapted by the proposed IPG algorithm are much lower than those of the ANF-I that is adapted by IPG algorithm of [4]. In addition,

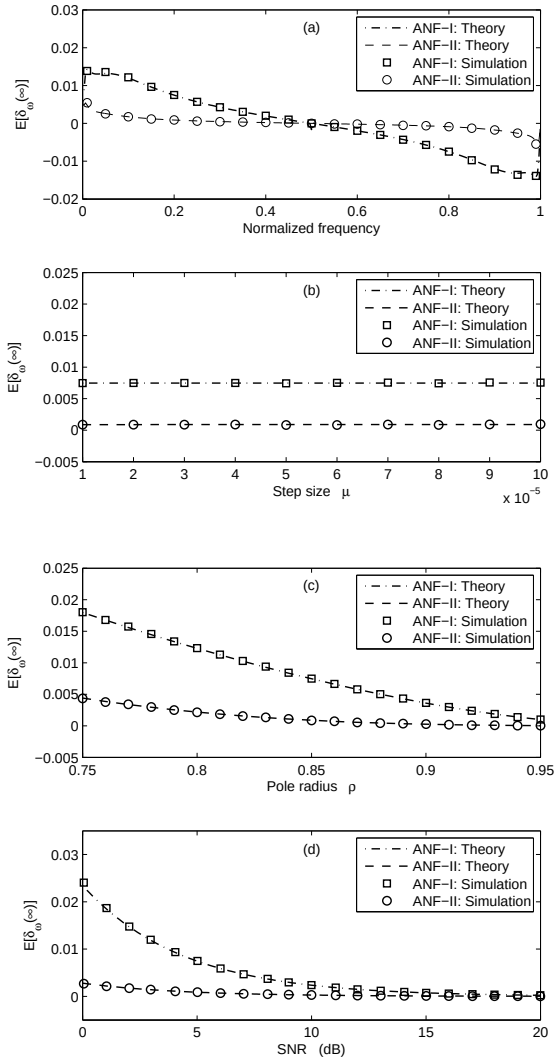

Fig.2: *Steady-state Performances of the DPG Algorithms. (a) Bias versus Input sinusoidal Frequency. (b) Bias versus Step Size. (c) Bias versus Pole Radius. (d) Bias versus SNR.*

these analytical results are very close to their simulated results.

6.2 Bias Behaviors of DPG Algorithms

This section will demonstrate the steady-state performances of the ANF-II whose notch frequency is adjusted by the proposed DPG algorithm of (27). In addition, the results will be compared with those results of the ANF-I that is adjusted by the DPG algorithm [8] under the same parameters.

The bias versus the input sinusoidal frequency is illustrated in Fig. 2 (a). To achieve the compared results, the parameters are defined as follows: $\mu = 5\times 10^{-5}$, $\rho = 0.85$, SNR = 5dB and $\theta = \pi/10$. Fig. 2 (b) shows the bias versus the step size of the algorithms by defining the parameters to be $\omega_o = 0.2\pi$, $\rho = 0.85$, SNR = 5dB and $\theta = \pi/10$. Furthermore, Fig. 2 (c) depicts the bias versus the pole radius of both filters that are adapted by their algorithms. To obtain the compared results, the parameters are determined in values of $\omega_o = 0.2\pi$, $\mu = 5 \times 10^{-5}$, SNR = 5dB and $\theta = \pi/10$. In addition, the bias versus the SNR is shown in Fig. 2 (d) by defining the parameters as follows: $\omega_o = 0.2\pi$, $\mu = 5 \times 10^{-5}$, $\rho = 0.85$ and $\theta = \pi/10$.

As illustrated in Fig. 2 (a) to Fig. 2 (d), they have implied that the ANF-II which its notch frequency is adjusted by proposed algorithm has lower steady-state bias. In addition, the analytical results are very fit to their simulated results.

Since such a structure of the ANF-II which poles precede zeros, the gradient noises of the proposed algorithms are rather low. Thus, the cross correlations of r_{12} and r_{34} in the steady state of the algorithms are quite low and these lead to low steady-state bias properties.

6.3 Stability Bound Results

For the simulation processes, the parameters are determined as $\omega_o = 0.2\pi$ and $\theta = \pi/10$. To obtain the results, 100 runs of the proposed algorithms are operated for each step-size value and each run employs the input signal with 10,000 samples. The step size will be increased from small value to large value until divergence and the previous step-size value will be accepted. The comparisons between analytical and simulated results of both algorithms by defining SNR = 10 dB and SNR = 0 dB are illustrated in Fig. 3 (a) and Fig. 3 (b), respectively.

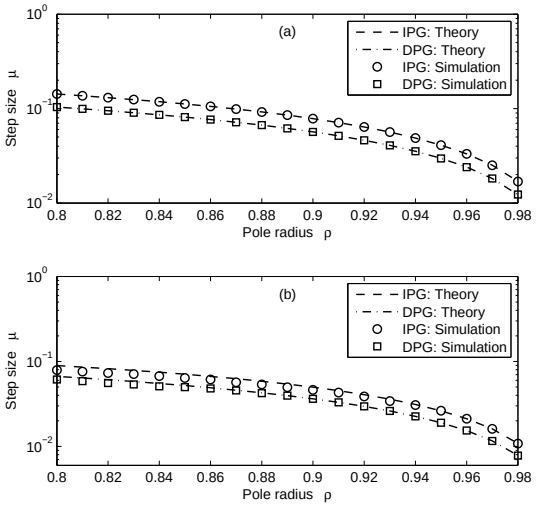

Fig.3: *Stability Bounds of the Proposed IPG and DPG Algorithms. (a) SNR = 10 dB. (b) SNR = 0 dB.*

They have been shown that the simulation results have the curves accordant to the analytical results

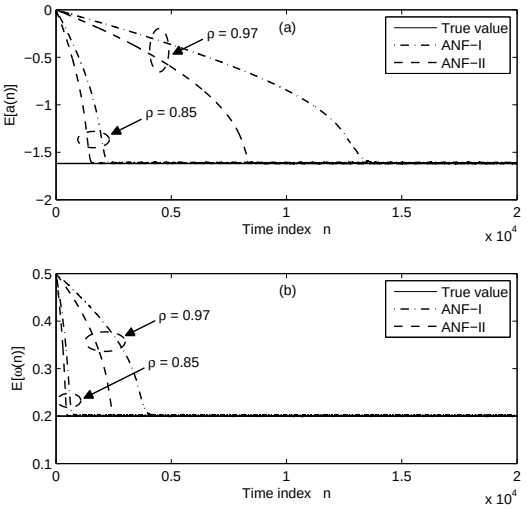

Fig.4: *Convergent Properties of the IPG and DPG Algorithms. (a) IPG Algorithms. (b) DPG Algorithms.*

for high SNR value while both results are slightly different in low SNR. Therefore, the stability bounds of the algorithms can be approximately indicated by this approach.

6.4 Convergent Behavior Results

In this section, convergent behaviours of the proposed algorithms which adapt the ANF-II are demonstrated by simulation processes. Moreover, these results are also compared with those results of the algorithms [4, 8] that adapt the ANF-I by defining the same parameters. To obtain the results, the parameters are defined as follows: $\omega_o = 0.2\pi$, $\mu = 0.005$, $\theta = \pi/10$, SNR = 5 dB and 100 runs. Fig. 4 (a) shows the compared results of the ANF-II and ANF-I that the coefficients are updated by their IPG algorithms with the pole radius $\rho = 0.85$ and $\rho = 0.97$, respectively. The convergent properties of the ANF-I and ANF-II which are adapted by their DPG algorithms are depicted in Fig. 4 (b) by defining $\rho = 0.85$ and $\rho = 0.97$.

Although these algorithms are based on the same plain-gradient estimation, it has revealed that the ANF-II structure produces quite good convergent speed referred to the ANF-I structure with the pole radius near one.

7. CONCLUSION

In this paper, performance of the ANF-II structure which is adapted by the proposed IPG and DPG algorithms has been analysed. The steady-state bias properties of the algorithms have been derived in closed form. The simulations have been performed for comparing these results with the analytical results in order to confirm validity of the theoretical analyses. Moreover, these results have also been compared with those results of the ANF-I structure that is adapted by the IPG algorithm of [4] and the DPG algorithm of [8] under the same parameters. Clearly, the ANF-II has provided the steady-state performance over the ANF-I because such a direct form II structure produces lower gradient noise of their plain-gradient estimation algorithms. Furthermore, the stability bounds of the proposed algorithms have been analysed to find the solutions and these have been verified by their simulation results as well. In addition, the compared results from the simulation processes have shown that the convergent properties of the proposed algorithms which adapt the ANF-II structure are faster than those properties of the algorithms that update the ANF-I structure.

References

[1] A. Nehorai, "A minimal parameter adaptive notch filter with constrained poles and zeros," *IEEE Trans. Acoust., Speech, Signal Process.*, vol.ASSP-33, no.4, pp. 983-996, Aug, 1985.

[2] J. F. Chicharo and T. S. Ng, "Gradient-based adaptive IIR notch filtering for frequency estimation," *IEEE Trans. Acoust., Speech, Signal Process.*, vol.38, no.5, pp. 769-777, May, 1990.

[3] S.-C. Pei and C.-C. Tseng, "Adaptive IIR notch filter based on least mean p-power error criterion," *IEEE Trans. Circuits, Syst.*, vol.40, no.8, pp. 525-529, Abbrev. Aug, 1993.

[4] Y. Xiao, Y. Takeshita and K. Shida, "Steady-state analysis of a plain gradient algorithm for a second-order adaptive IIR notch filter with constrained poles and zeros," *IEEE Trans. Circuits Syst. II.*, vol.48, pp. 733-740, July, 2001.

[5] Y. Xiao, R. K. Ward and A. Ikuta, "Performance analysis of the sign algorithm for a constrained adaptive IIR notch filter," *IEEE Trans. Signal Process.*, vol.57, no.7, pp. 1846-1858, July, 2003.

[6] W. Leotwassana, R. Punchalard and W. Silaphan, "Adaptive howling canceller using adaptive IIR notch filter: Simulation and implementation," in *IEEE Int. Conf. Neural Network and Signal Process.*, pp. 848-850, Dec, 2003.

[7] Y. Chen, P. Willett and Q. Zhu, "Frequency tracking in optical Doppler tomography using an adaptive notch filter," *Biomed Opt. J.*, vol.12, no.1, pp. 1-16, 2007.

[8] J. Zhou and G. Li, "Plain gradient-based direct frequency estimation using second-order constrained adaptive IIR notch filter," *Electron. Lett.*, vol.50, no.5, pp. 351-352, Mar, 2004.

[9] R. Punchalard, A. Lorsawatsiri, J. Koseeyaporn, P. Wardkein and A. Roeksabutr, "Adaptive IIR notch filters based on new error criteria," *Signal Processing.*, vol.88, pp. 685-703, 2008.

[10] R. Punchalard, A. Lorsawatsiri, W. loetwassana,

J. Koseeyaporn, P. Wardkein and A. Roeksabutr, "Unbiased plain gradient algorithm for adaptive IIR notch filter with constrained poles and zeros," *IEEE TENCON2007.*, pp. 1-4, 2007.

[11] W. Loetwassana, R. Punchalard, J. Koseeyaporn, and P. Wardkein, "Unbiased Plain Gradient Algorithn for a Second-order Adaptive IIR Notch Filter with Constrained Poles and Zeros," *Signal Processing.*, vol.90, no.8, pp. 2513-2520, Aug, 2010

[12] D. V. Bhaskar Rao and S. Y. Kung, "Adaptive notch filtering for the retrieval of sinusoids in noise," *IEEE Trans. Acoust., Speech, Signal Process.*, vol.ASSP-32, no.4, pp. 791-802, Aug. 1984.

[13] M. Ferdjallah and R. E. Barr, "Adaptive digital notch filter design on the unit circle for the removal of powerline noise from biomedical signals," *IEEE Trans. Biomedical Eng.*, vol.41, no.6, pp. 529-536, Jun, 1994.

[14] Y. C. Lim, Y. X. Zou and N. Zheng, "A piloted adaptive notch filter," *IEEE Trans. Signal Process.*, vol.53, no.4, pp. 1310-1323, Apr, 2005.

[15] L. Tan and J. Jiang, "Simplified gradient adaptive harmonic IIR notch filter for frequency estimation and tracking," *American Journal of Signal Process.*, vol.5, no.1, pp. 6-12, 2015.

Wuthiporn Loedwassana received the B. Eng., M. Eng. and D. Eng. degrees from King Mongkut's Institute of Technology Ladkrabang (KMITL) in 1993, 2003 and 2011, respectively. He is currently lecturer at Mahanakorn University of Technology. His research interests include adaptive signal processing, analog and digital filters design and digital signal processing for telecommunications.